Citation: Cell Death and Disease (2013) 4, e484; doi:10.1038/cddis.2013.13

www.nature.com/cddis

Conformational altered p53 affects neuronal function: relevance for the response to toxic insult and growth-associated protein 43 expression

L Buizza*[,1], C Prandelli[1], SA Bonini[1], A Delbarba[2], G Cenini[1], C Lanni[3], E Buoso[3], M Racchi[3], S Govoni[3], M Memo[1] and D Uberti[1]

The role of p53 in neurodegenerative diseases is essentially associated with neuronal death. Recently an alternative point of view is emerging, as altered p53 conformation and impaired protein function have been found in fibroblasts and blood cells derived from Alzheimer's disease patients. Here, using stable transfected SH-SY5Y cells overexpressing APP751wt (SY5Y-APP) we demonstrated that the expression of an unfolded p53 conformation compromised neuronal functionality. In particular, these cells showed (i) augmented expression of amyloid precursor protein (APP) and its metabolites, including the C-terminal fragments C99 and C83 and β-amyloid peptide (ii) high levels of oxidative markers, such as 4-hydroxy-2-nonenal Michael-adducts and 3-nitro-tyrosine and (iii) altered p53 conformation, mainly due to nitration of its tyrosine residues. The consequences of high-unfolded p53 expression resulted in loss of p53 pro-apoptotic activity, and reduction of growth-associated protein 43 (GAP-43) mRNA and protein levels. The role of unfolded p53 in cell death resistance and lack of GAP-43 transcription was demonstrated by $ZnCl_2$ treatment. Zinc supplementation reverted p53 wild-type tertiary structure, increased cells sensitivity to acute cytotoxic injury and GAP-43 levels in SY5Y-APP clone.

Cell Death and Disease (2013) **4,** e484; doi:10.1038/cddis.2013.13; published online 7 February 2013
Subject Category: Neuroscience

Introduction

p53 is a pleiotropic protein involved in a very large number of biological processes, including cell cycle regulation, cell differentiation and apoptosis.[1] Regulation of p53 activity is crucial in determining cellular outcome: p53 promotes DNA repair or induces apoptosis upon cytotoxic insults.[2] The cell fate depends on the damage degree and on the cellular phenotype.[3]

In central nervous system, p53 signaling has been often associated with neuronal death.[4–6] While, during brain development, p53 is required to eliminate neuron excess in order to ensure the correct neuronal cytoarchitecture,[7] in mature neurons p53-mediated cell death is correlated with neurodegeneration.[8] Indeed, several data demonstrated that different excitotoxic insults induced apoptosis in a p53-dependent manner, leading to progressive decline of neuronal functionality and finally cellular death.[9–11] Furthermore, increased p53 immunoreactivity associated with neuronal death was observed in models of cerebral ischemia, traumatic brain injury and epilepsy.[8,12] In agreement with these data, many studies demonstrated that inhibition of p53 prevented cell death in a variety of neurodegenerative models.[13,14]

Interestingly, an intriguing non-apoptotic role for p53 has been proposed by recent research carried out by Di Giovanni and co-workers.[15] Surprisingly, p53 is required for axonal outgrowth in primary neurons, as well as for axonal regeneration following neuronal injury in mice, probably through different post-translational pathways. Loss of p53 activity, induced by specific p53 inhibitors or by transfection with dominant-negative forms of p53, compromises synaptic remodeling, leading to neuronal dysfunction.[16] p53 transactivates neuronal growth-associated protein 43 (GAP-43), a protein involved in neuronal morphology.[17] This protein is the major constituent of the growth-cone and has a key role in guiding the growth of axons and modulating the formation of new connections.[18] Downregulation of GAP-43 expression may reflect an important molecular lesion that precedes and progresses with widespread synaptic disconnections and neurodegeneration.[19]

Hence, the role of p53 in neurodegenerative diseases could be revised, because an impairment, rather than an excessive activation, of p53 intracellular signaling may be involved in the development of neuronal dysfunction. Our group demonstrated that conformational changes in p53 tertiary structure was present in peripheral cells (that is, fibroblasts and blood cells) derived from Alzheimer's (AD) patients.[20–22] In addition, Serrano *et al.*,[23] showed that old AD transgenic mice APPswe/PS1-A246E exhibited a mutated p53 conformation and were more prone to develop brain tumor after carcinogen

[1]Department of Molecular and Translational Medicine, University of Brescia, Brescia, Italy; [2]Diadem Ltd, Spin off of University of Brescia, Brescia, Italy and [3]Department of Drug Sciences, Centre of Excellence in Applied Biology, University of Pavia, Pavia, Italy
*Corresponding author: Dr L Buizza, Department of Molecular and Translational Medicine, University of Brescia, Viale Europa 11, 25123 Brescia, Italy. Tel: +39 030 3717 509; Fax: +39 030 3717 529; E-mail: laura.buizza@med.unibs.it
Keywords: oxidative stress; Alzheimer's disease; p53; GAP-43; protein conformation
Abbreviations: AD, Alzheimer's disease; APP, amyloid precursor protein; GAP-43, growth-associated protein 43; HNE, 4-hydroxy-2-nonenal; 3NT, 3-nitrotyrosine; NQO1, NADH quinone oxidoreductase; Pif, pifithrin-α; RA, retinoic acid
Received 06.8.12; revised 04.12.12; accepted 20.12.12; Edited by A Verkhratsky

20-methycholanthrene injection, compared with younger mutants and with wild-type counterparts of the same age.

AD is a slowly progressing disorder characterized by memory loss and cognitive decline.[24]

Abnormal production and deposition of Aβ peptides in the brain is one of the most reliable causes of AD pathogenesis.[25] Aβ derives from amyloidogenic processing of a protein named amyloid precursor protein (APP), whose gene mutations are correlated with familiar cases of AD.[26] In addition, reduced GAP-43 expression was observed in AD brain,[27–29] suggesting a synaptic disfunction in the development of the disease.

Thus, this study investigated the contribution of p53 conformational changes to neuronal dysfunction and neuronal death in AD, using a human neuroblastoma cell line SH-SY5Y steadily transfected with APP751-wild-type (called SY5Y-APP). We demonstrated that SY5Y-APP cells showed an impairment in neuronal responses against acute toxic insults and a reduction of GAP-43 levels, due to a lack of p53 trascriptional activity.

Results

Characterization of SY5Y-APP clone. SY5Y-APP cells expressed increased APP mRNA (Figure 1a), and protein levels (Figure 1b) as measured by real-time PCR (RT-PCR) and western blot analysis with 22C11 antibody (that recognized N-terminus of APP), respectively. In addition, we demonstrated an enhanced APP metabolism in SY5Y-APP clone if compared with mock cells. Western blot analysis performed with 6E10 antibody (recognizing the fragment 1–17 of Aβ) revealed exclusively in SY5Y-APP clone the presence of different bands corresponding to different APP metabolic products: APP full-length of about 150 kDa; a band at 100 kDa corresponding to immature protein, one at 50 kDa, reported in litterature as a metabolic product of amyloidogenic pathway;[30] and finally smear bands around 15-8 kDa corresponding to C-terminus fragments (βCTFs). Immunostaining with APP-C-terminus antibody identified two bands corresponding to C99 and C83 fragments that were significantly more intensive in SY5Y-APP clone in comparison with mock cells. Figure 1c showed confocal microscopy analysis with a specific antibody against Aβ peptide. Cells overexpressing APP showed an evident accumulation of β-amyloid staining.

SY5Y-APP cells showed a high oxidative stress and conformational altered p53 expression. Recent data point an intriguing relationship between Aβ and oxidative stress.[31]

Oxidative stress was evaluated by measuring the expression of different oxidative markers; especially, we focused on protein-bound 4-hydroxy-2-nonenal (HNE), a product of lipid peroxidation,[32] and 3-nitrotyrosine (3NT), which, via peroxynitrite, results in the addition of a nitro-group to tyrosine residues.[33] HNE and 3NT products were found significantly enhanced in SY5Y-APP clone in relation with mock cells (Figures 2a and b), suggesting the presence of an increased oxidative environment in this clone.

It is well recognized that p53 is particularly sensitive to cellular redox modulation.[34] At this regards, we recently demonstrated a correlation between oxidative stress and nitrated-p53 in blood peripheral cells derived from sporadic and familiar AD patients.[35] Nitration of p53-tyrosine residues was demonstrated to change its tertiary structure in an unfolded conformation.[35] In this study, SY5Y-APP and mock cells were immunoprecipitated with two conformationally specific antibodies (PAb1620 antibody, direct towards

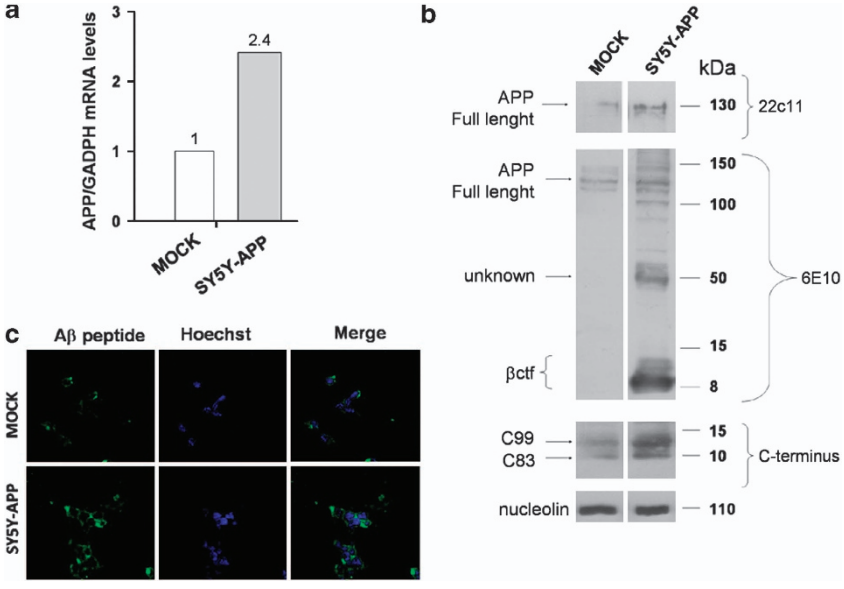

Figure 1 Characterization of SY5Y-APP clone. mRNA and protein extracts were obtained from Mock cells and SY5Y-APP clone. (**a**) Q-RT-PCR was performed using RNA extracted from mock and SY5Y-APP cells to evaluate APP expression levels. Data were expressed as fold change of target gene expression, normalized to the internal control gene (*GAPDH*). Data were analyzed according to the comparative Ct method. (**b**) Western blot analysis was carried out with different anti-APP antibodies (22C11 against N-terminal amino acids; 6E10 against fragment 1–17 of Aβ and C-terminus against the last C-terminus nine amino acids). Anti-nucleolin antibody was used to normalize protein content. (**c**) Confocal microscopy analysis was performed using an anti-Aβ peptide on mock and SY5Y-APP cells

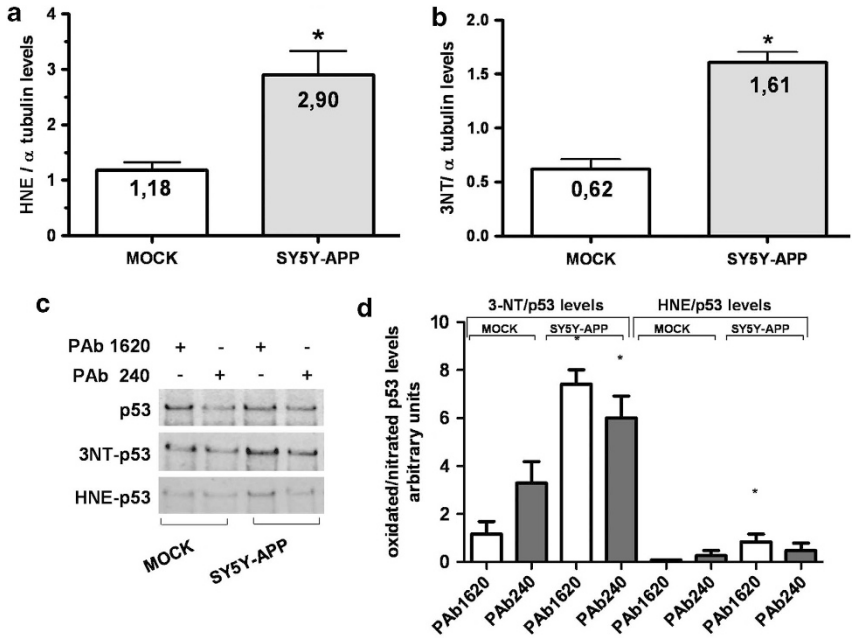

Figure 2 Elevated oxidative markers in SY5Y-APP cells. (**a** and **b**) Mock cells and SY5Y-APP clone were processed for measurement of oxidative markers by Dot blot analysis using specific antibodies against protein-bound-HNE and 3NT. α-tubulin expression was used to normalize protein content. Data are represented as mean ± S.E.M. of at least three different experiments. $^{*}P<0.05$ MOCK *versus* SY5Y-APP; $^{**}P<0.001$ MOCK *versus* SY5Y-APP. (**c**) Immunoprecipitated experiments with two conformational specific anti-p53 antibodies that recognized wild-type (PAb1620) and unfolded (PAb240) p53 state. Immunoprecipitated p53 was then loaded on 10% SDS-PAGE gel and immunoblotted with anti-p53; anti-HNE and anti-3NT antibodies. (**d**) Quantitative analysis of 3NT/HNE-p53 positive bands were done on three different immunoblots derived from three different cell preparations. Data were expressed as the ratio between oxidated/nitrated-p53 intensity band on the corresponding p53 conformational isoforms

wild-type form of the protein, competent for DNA binding and PAb240, which recognizes an epitope cryptic when the protein is in its folded form and accessible when the protein undergoes conformational changes[36]), and then blotted with a polyclonal anti-p53 antibody. Cells transfected with empty vector expressed mainly wild-type p53, as demonstrated by the reactivity with PAb1620 and the poor responsiveness to PAb240. SY5Y-APP cells showed a band reactive to PAb240 antibody in association with PAb1620-positive band (Figure 2c). Immunoprecipitated extracts were also immunoblotted with anti-HNE or anti-3NT antibodies to investigate the degree of oxidation/nitration of p53 molecule in the two conformations. As shown in Figure 2c, HNE-p53 band was evident especially in the SY5Y-APP sample immunoprecipitated with PAb1620 (wt conformation). Differently, a weak 3NT-p53-positive band was observed in mock extracts immunoprecipitated with PAb240 antibody (unfolded p53), whereas in SY5Y-APP cells, nitration of tyrosine residues was more evident in both wild-type (PAb1620) and unfolded (PAb240) conformations. Quantitative analysis of 3NT/HNE-p53-positive bands were done on three different immunoblots derived from three different cell preparations. Data were expressed as the ratio between 3NT/HNE-p53 intensity band on the corresponding p53 conformational isoforms. As reported in Figure 2d, 3NT-unfolded and 3NT-wild-type p53 levels were statistically increased in SY5Y-APP clone in comparison with mock cells. At variance, SY5Y-APP clone showed high HNE-p53 expression, especially when the protein was in its native conformation.

SY5Y-APP cells resulted less sensitive to acute toxic stress. To investigate the consequence of unfolded p53 expression on cellular responses upon a toxic insult, SY5Y-APP and mock cells were exposed to a brief pulse of H_2O_2 (see methods section). H_2O_2 induced a reduction of cell viability of about 50% in mock cells, whereas SY5Y-APP cells resulted more resistant to the oxidative insult (Figure 3a). As expected, in mock cells oxidative injury induced p53 pathway activation within few hours: p53 protein expression increased already at 1 h after the H_2O_2 stimulus and remained high at least until 4 h; p21 protein levels, a target gene of p53, significantly increased at 4h following insult. In SY5Y-APP cells, p53 intracellular pathway was impaired. We found the lack of an increased p53 expression (that was anyway already high in basal condition) and p21 expression (Figure 3b). p53 transcriptional activity was also evaluated by transfecting cells with p53AIP1-luciferase apoptotic promoter. As shown in Figure 3c, p53AIP1-luciferase activity was induced by doxorubicin treatment in mock cells. At variance, in SY5Y-APP clone p53 activity induced by noxious insult was significantly impaired. Notably, H_2O_2 and doxorubicin injuries did not affect p53 unfolded conformation in mock and SY5Y-APP cells, while these toxic insults induced, as expected, the increased expression of p53 wild-type only in mock cells (data not shown).

SY5Y-APP cells showed GAP-43 dependent impairment in axonal outgrowth. Accumulating evidence suggested a role of p53 in neuronal maturation and axonal outgrowth,

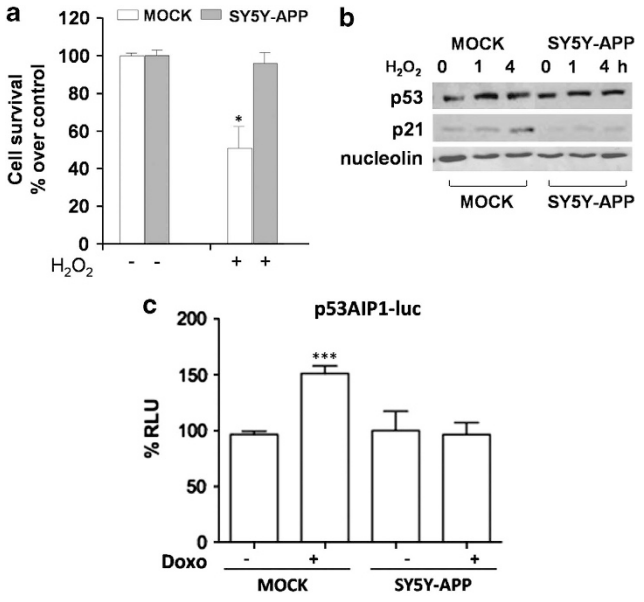

Figure 3 SY5Y-APP cells were less sensitive to toxic insults. Cells were exposed to H_2O_2 pulse (5 min), followed by incubation with fresh medium for different times (1, 4 and 24 h). (**a**) Cell viability was evaluated 24 h after oxidative insults by MTT assay. Data were expressed as % of cell survival *versus* respective controls. Values are the mean ± S.E.M. of three different experiments. $^*P<0.001$ H_2O_2- treated mock *versus* control mock. (**b**) Protein extracts derived from mock and SY5-APP cells at 1 and 4 h after H_2O_2 pulse were processed for western blot analysis with anti-p53, anti-p21 antibodies. Nucleolin was used for sample normalization. (**c**) Mock and SY5Y-APP cells were transfected with p53AIP1-luc promoter and 18 h later they were treated with 50 μM doxorubicin (Doxo). As much as 24 h after toxic insult, cells were processed for the measurement of luciferase activity. Data were expressed as % of relative luminescence unit (RLU) $^{***}P<0.0001$ Doxo-treated mock *versus* control mock

transactivating *GAP-43* gene.[15,37,38] Hence, we wonder whether in SY5Y-APP cells, that expressed unfolded p53, the expression of GAP-43 was compromised. For this purpose, SY5Y-APP and mock cells were evaluated in term of GAP-43 mRNA and protein levels. RT-PCR demonstrated a fivefold reduction of GAP-43 mRNA in SY5Y-APP clone in comparison with mock cells (Figure 4a). In addition western blot analysis reflected the RT-PCR results, showing a significant decrease of GAP-43 protein levels if compared with mock cells (Figure 4b). Interestingly the expression of β-III tubulin, a component of neuronal cytoskeleton, was comparable in the SY5Y-APP and mock cells (Figure 4b). The relevance of a GAP-43 downregulation in SY5Y-APP clone was shown by the treatment with retinoic acid (RA). In particular, mock cells and SY5Y-APP were exposed to RA for 48 h. RA exposure slightly increased GAP-43 expression in SY5Y-APP cells (Figure 4c). However, this increase was not correlated with p53 transcriptional activity, as it was not prevented by 200 nM pifithrin-α (Pif), a specific p53 inhibitor. The efficacy of pif-treatment was confirmed by the reduction in mock cells of GAP-43 expression, whose gene is a target gene of p53.[15]

Figure 4d showed representative confocal images that evidence neurite elongation and growth-cone formation in mock cells after 48 h RA exposure. As expected, growth-cone area was GAP-43-positive in these cells. At variance SY5Y-APP showed RA-induced neurite outgrowth, but a poor growth-cone expansion with a weak GAP-43 staining (Figure 4d). Retinoic-acid treatment had no effects on both wild-type and unfolded p53 in SY5Y-APP cells. Mock cells responded to RA treatment with an increased expression of p53 wild-type isoform (data not shown). This latter result was in line with different studies that demonstrated a high expression of p53 after RA treatment, suggesting its role in neurite outgrowth and neuronal differentiation.[39,40]

SY5Y-APP phenotype was restore by zinc chloride supplementation. p53 tertiary structure is endowed with high flexibility.[36] Different compounds influence p53 conformational state that shifts from wild-type to unfolded phenotype and vice versa.[36] For example, zinc chloride restores p53 wild-type conformation, stabilizing the core domain.[41] At this regards, we exposed SY5Y-APP and mock cells to zinc supplementation at the concentration of 100 μM for 24 h and p53 conformational state was evaluated by enzyme-linked Immunosorbent assay (ELISA) with PAb1620 and PAb240 antibodies.

The expression of unfolded p53 (PAb240 positive) was significantly higher in SY5Y-APP clone than levels found in mock cells (Figure 5a). The treatment with zinc chloride mainly reduced the levels of PAb240 positive-p53 in SY5Y-APP cells (Figure 5a). This effect was evident also in mock cells showing a statistically significant reduction of unfolded quote after zinc supplementation (Figure 5a). However, a decrease of total p53 protein expression was observed after zinc treatment in both SY5Y-APP and mock cells (data not shown).

Zinc chloride also decreased the expression of PAb1620-positive p53 in cells overexpressing APP (Figure 5b). In fact, a huge amount of wild-type p53 was expressed in SY5Y-APP cells if compared with mock cells. This result is consistent with immunoprecipitation results reported in Figure 2c, and with confocal analysis performed with PAb1620 and PAb240 antibodies (data not shown).

To test cell viability upon oxidative insult, the experiments foresaw 24 h zinc pre-treatment in the absence or presence of the p53 inhibitor Pif, followed by the acute oxidative insult. As depicted in Figure 5c, mock cells showed a decrease of $\sim$40% in cells survival, after H_2O_2 insult. The same result was obtained in mock cells treated with zinc-chloride. Finally, pif-treatment, alone or in association with zinc supplementation, worked properly, precluding cell death. On the contrary, SY5Y-APP cells showed a 20% decrease in cell survival after H_2O_2 pulse. Zinc pre-treatment rendered this clone more vulnerable to oxidative injury with a death estimated of $\sim$50%. When zinc pre-treatment was combined with pif pre-exposure, H_2O_2-induced cell death was prevented in SY5Y-APP cells (Figure 5d), suggesting that zinc rescued wild-type p53 conformation and pro-apoptotic activity.

Zinc supplementation also caused a 50% increase in GAP-43 mRNA levels in SY5Y-APP clone, but not in mock cells (Figure 6a). Furthermore, confocal microscopy analysis, confirmed the increased protein expression of GAP-43 induced by zinc supplementation in SY5Y-APP cells (Figure 6b).

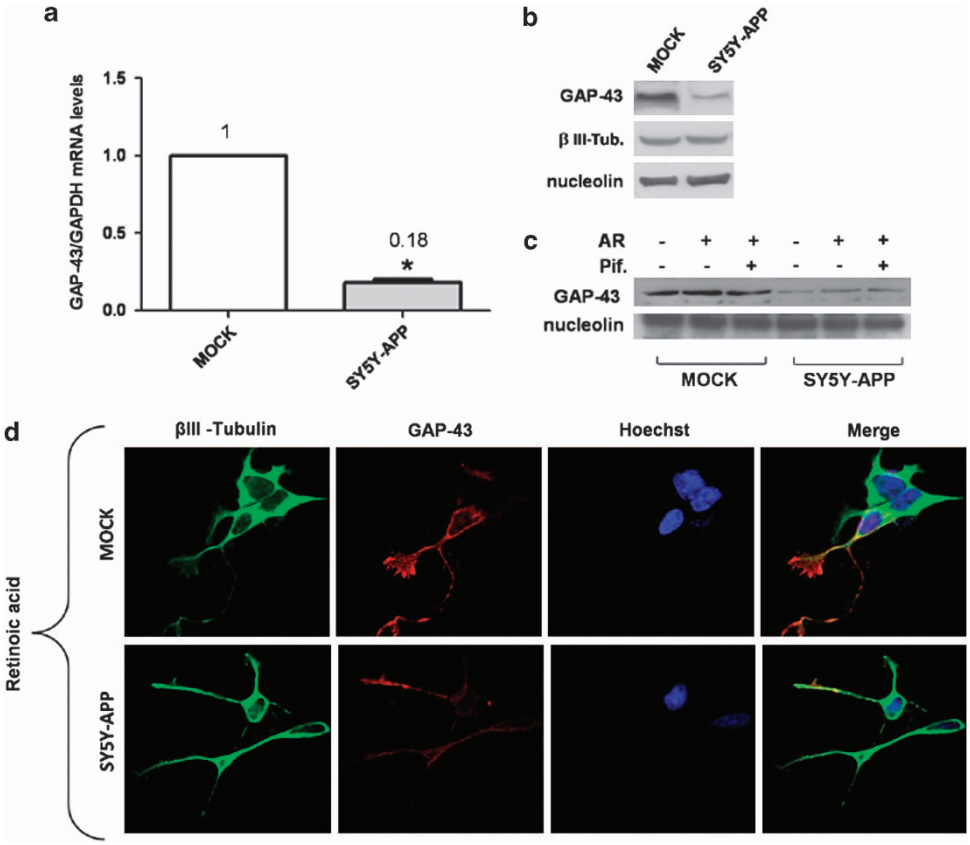

Figure 4 GAP-43 expression was decreased in SY5Y-APP cells. (**a**) Q-RT-PCR was performed using RNA extracted from mock and SY5Y-APP cells to evaluate GAP43 expression levels. Data were expressed as fold change of target expression, normalized to the internal control gene (*GAPDH*). Data were analyzed according to the comparative Ct method. (**b**) Protein extracts derived from mock and SY5Y-APP cells were processed for western blot analysis carried out with anti-GAP-43 and anti-βIII Tubulin antibodies. Nucleolin was used for sample normalization. (**c**) Mock and SY5Y-APP cells were exposed to RA in the presence or absence of Pif. Forty-eight hours later cells were processed for western blot analysis using anti-GAP-43 antibody. Nucleolin was for sample normalization; pif-treatment efficacy was confirmed in mock cells by the reduction of GAP-43 expression, whose gene is a target gene of p53. (**d**) Confocal microscopy analysis with anti-GAP43 and anti-β III tubulin antibodies was performed on 48 h RA-treated cells

To investigate the affinity of wild-type p53 protein for the GAP-43 promoter elements, chromatin immunoprecipitation assay (ChIP) was performed, after treating SY5Y-APP cells with $ZnCl_2$ in the presence or absence of RA. As shown in Figure 6c, in basal condition p53 was mostly in unfolded conformation and did not occupy GAP-43 promoter region. Differently, treatment with $ZnCl_2$ restored wild-type p53 that in this conformation was found to occupy the GAP-43 promoter. Retinoic-acid exposure did not substantially influenced the effect of zinc chloride.

Moreover, when SY5Y-APP cells were differentiated by RA in the presence of zinc-chloride, extensive growth cone area GAP-43 positive was observed. Whereas in the absence of zinc supplementation, RA induced in this clone only neurite elongation, indicative of incomplete differentiation (Figure 7).

Discussion

In this study, we developed a clone of human neuroblastoma cell line SH-SY5Y overexpressing APP751wt. This clone appeared suitable to investigate molecular mechanisms involved in AD. Indeed, if related to mock cells, SY5Y-APP clone showed (i) elevated APP mRNA and protein levels, (ii) increased expression of APP metabolites, among them CTFs C99 and C83 and (iii) enhanced Aβ peptide immunoreactivity.

Although 'Aβ cascade theory' is one of the most accredited hypothesis to explain the development of AD,[42] a growing body of evidence support a role of oxidative stress, as well as inflammation mechanisms in the pathogenesis of the disease.[43–45] It is anyway debated whatever increased oxidative stress could be a cause of Aβ load or vice versa Aβ itself may be a pro-oxidant agent.[46]

SY5Y-APP clone showed a high oxidative environment underlined by peculiar products of lipoperoxidation, such as HNE Michael-adducts and peroxynitrite addition to tyrosine residues, resulting in 3-nitro-tyrosine. This elevated oxidative environment affected also p53 structure. In SY5Y-APP clone, p53 is mainly present in unfolded conformation, as showed by using two-specific conformational antibodies that discriminate folded (PAb1620) *versus* unfolded (PAb240) p53 state. The contribution of amyloidogenic metabolic products affecting p53 conformational change towards an unfolded phenotype was also supported by treating mock cells with nM concentration of Aβ (Supplementary Figure 1A). In addition, Aβ pre-treatment at different concentration ranging from 0.02 to 10 nM protected the cells against oxidative insult

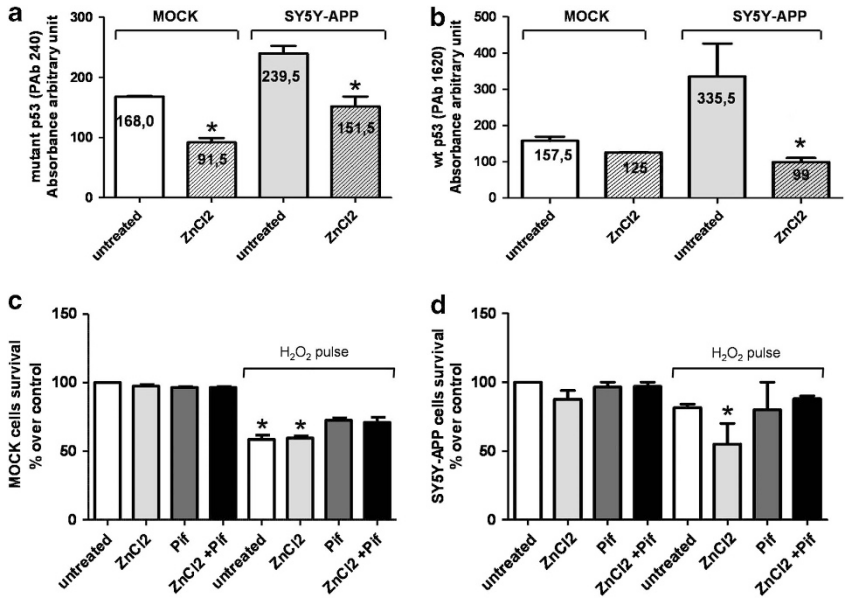

Figure 5 $ZnCl_2$ restored p53 wild-type conformation and SY5Y-APP cell sensitivity against oxidative insult. Cells were treated with 100 μM $ZnCl_2$ for 24 h and then processed for p53 conformational analysis and cell viability. (**a** and **b**) ELISA immunoassay carried out with PAb240 (unfolded p53) (**a**) and PAb1620 (wild type p53) (**b**) antibodies. (**c** and **d**) After 24 h $ZnCl_2$ pretreatment, mock (**c**) and SY5Y-APP (**d**) cells were exposed to H_2O_2 pulse (5 min) in the presence or absence of the p53 inhibitor, Pif, followed by incubation with fresh medium for additional 24 h. Cell viability was evaluated by MTT assay. Data were expressed as % of cell survival *versus* respective controls. Values were the mean ± S.E.M. of three different experiments. *$P < 0.001$ $ZnCl_2$ followed by H_2O_2-treated SY5Y-APP cells *versus* $ZnCl_2$ pre-treated SY5Y-APP cells

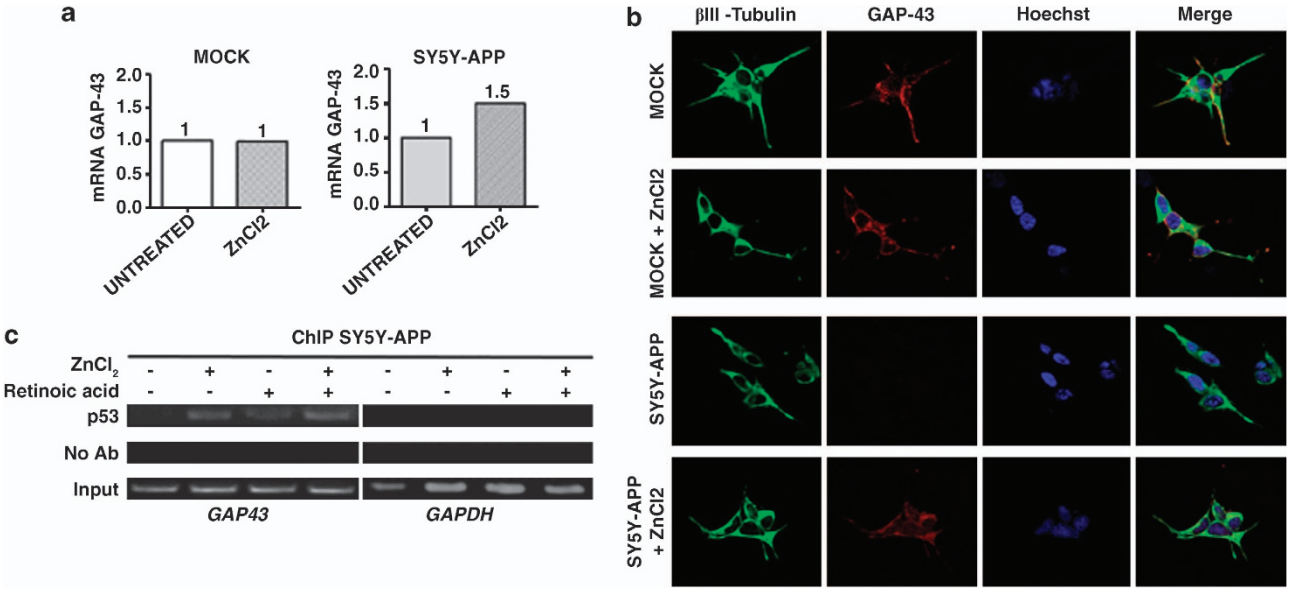

Figure 6 $ZnCl_2$ restored p53 transcriptional activity and GAP-43 expression. (**a**) Mock and SY5Y-APP cells were treated with 100 μM $ZnCl_2$ for 24 h and then cells were processed for Q-RT-PCR. Data were expressed as fold change of GAP43 expression, normalized to the internal control gene (*GAPDH*). Data were analyzed according to the comparative Ct method. (**b**) Mock and SY5Y-APP cells were treated with 100 μM $ZnCl_2$ for 24 h and then cells were processed for confocal microscopy analysis. Cells were fixed in methanol, immunostained with anti-βIII tubulin and anti-GAP-43 antibodies, and analyzed to confocal microscopy. (**c**) SY5Y-APP cells untreated and treated with $ZnCl_2$ in the presence or absence of RA were processed for ChIP analysis. Cells were crosslinked with formaldehyde and immunoprecipitated with the polyclonal anti-p53 full length antibody (FL-393). PCR analyses were performed on the immunoprecipitated DNA samples using specific primers for the GAP-43 promoter. A sample representing linear amplification of the total input chromatin (Input) was included as control. Additional controls included immunoprecipitation performed with nonspecific immunoglobulins (no Ab). Amplification of GADPH housekeeping gene was used as control of p53-binding specificity to the GAP43 promoter

(Supplementary Figure 1B). This results were in line with our previous data on human fibroblasts and HEK cells.[47–49]

This unfolded structure in SY5Y-APP cells was, at least in part, the results of nitration to tyrosine residues of p53 molecule. Tyrosine-residues nitration was evident in both wild-type and unfolded p53 conformation. This is plausible as the p53 molecule contains 15 tyrosine residues, and 11 of them are inside the highly flexible DNA-binding domain.[50]

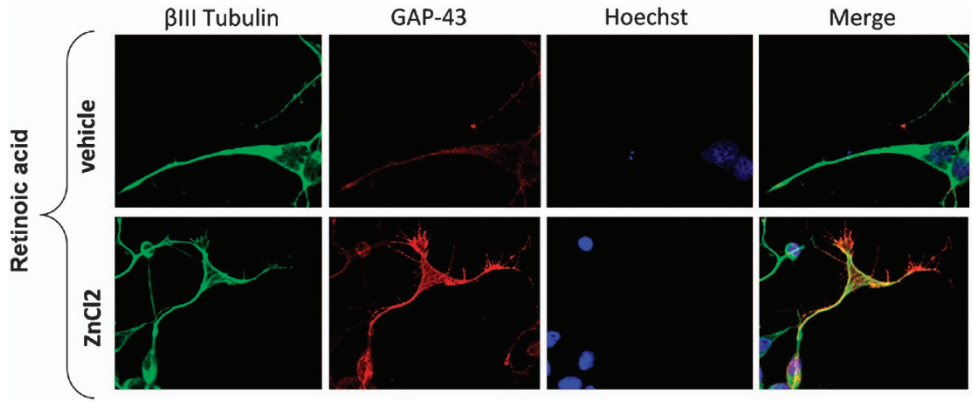

Figure 7 $ZnCl_2$ restored RA-induced growth cone in SY5Y-APP cells. Cells were treated with 10 μM RA for 48 h. Confocal microscopy was performed with anti-β III tubulin, anti-GAP-43 antibodies

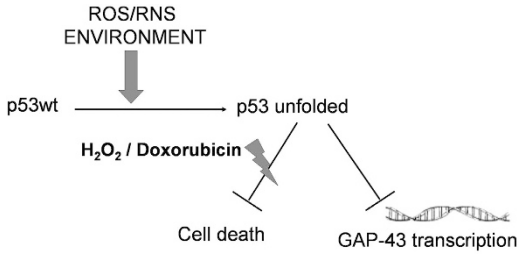

Figure 8 Schematizion of a proposed molecular cascade

Probably, upon a certain degree of nitration or depending by selective nitrated tyrosines, p53 shifted from wild-type towards unfolded conformation. Similar results were found in immortalized lymphocytes derived from familiar and sporadic AD, as well as in cells derived from healthy donor treated with peroxynitrite-generating compound SIN-1.[35] According with our data, Calmels *et al.*[51] demonstrated that synthetic nitric oxide donors induce a conformational switch of wild-type p53 to the unfolded form, with loss of DNA-binding activity *in vitro*.

What is the relevance of unfolded p53 in neuron-like cells?

Firstly, our data showed that SY5Y-APP cells, as well as mock cells treated with Aβ, resulted more resistant to toxic insults in comparison with mock cells. In particular, upon toxic insults, mock cells responded by activating p53 intracellular signaling that lead to the transactivation of pro-apoptotic gene. On the contrary, in SY5Y-APP cells the lack of p53 pro-apoptotic properties was the result of the presence of high expression of unfolded isoform that stabilize and rendered unfunctional also the wt quote. This was not unexpected as it is well known that mutant p53 may exert a dominant negative effect by preventing wt p53 from binding to the promoter of its target genes.[52]

As in SY5Y-APP clone a redox unbalance was evident, we cannot exclude that NADH quinone oxidoreductase (NQO1), which is induced in pro-oxidant environment, can contribute to p53 accumulation in the cell. It is in fact demonstrated that NQO1 can bind to p53 in a NADH-dependent manner.[53] The effects of NQO1 may also explain that in SY5Y-APP cells wt/unfolded p53 are trapped in the cytoplasm after H_2O_2 insult (data not shown).

Apparently these results seem to be in contrast with numerous studies demonstrating a pro-apoptotic role of p53 upon oxidative stress in neurodegeneration.[8,11,54] However, in a wider context, we can speculate that this 'no-death' effect leads to an accumulation of defective neurons in the SNC and may contribute to neuronal dysfunction leading to the development of the disease. Consistent with our findings, Xu *et al.*[55] demonstrated a loss of p53 pro-apoptotic activity in cells overexpressing APP695wt. Moreover, Serrano *et al.*[23] demonstrated a significant increase of unfolded p53 in older AD transgenic mice when compared with younger APPswe/PS1A246E animals and wild-type counterparts of comparable age. They also demonstrated that when carcinogen 20-methylcholanthrene compound was injected in tg mice, they developed brain tumors faster and with higher incidence than the wild-type counterparts, suggesting impairment in apoptotic processes. Indeed, ROS may have at least two distinct roles on p53 functions depending on their insult degree. Acute oxidative damage induces p53 canonical pathway, followed by the transactivation of its target genes. On the other hand, an alteration in oxidative homeostasis, resulting in a subtoxic and chronic ROS exposure, may affect p53 tertiary structure and impair its function.[56]

It is well established that different compounds modulate p53 conformational state.[36,41] p53 is endowed with an high flexibility because of its DNA central domain that contains a divalent Zn atom coordinated with three cysteines (residues 176, 238, 242) and one histidine (residue 179). Zinc binding is crucial for the stabilization of p53 protein in folded conformation.[36] Exposure of wild-type p53 to metal chelators results in a rapid shift towards unfolded p53 isoform; this effect is accompanied by loss of DNA-binding activity.[36,57] Furthermore, Zn treatment at micromolar concentration incorporates within the protein and restores p53 wild-type PAb1620-positive conformation.[36,41] This effect was also evident in our experimental procedures, where when we treated SY5Y-APP cells with zinc chloride, p53 tertiary structure shifted from unfolded to wild-type conformation. In particular, 24 h 100 μM $ZnCl_2$, a concentration that did not affect APP levels and processing (data not shown), reduced the expression of unfolded p53; notably there is also a decrease of p53wt levels, after zinc supplementation. This is due to the high turnover of

the protein in native tertiary structure. $ZnCl_2$ pre-treatment reverted also the resistance to oxidative injury in SY5Y-APP cells, which resulted more prone to toxic insult. This effect was p53-dependent, as cell death was prevented by the specific p53 inhibitor Pif.

Very recently it has been found a new role of p53 protein that might promote neuronal maturation, as well as axon outgrowth and regeneration, following neuronal injury.[38] In particular Tedeschi *et al.*[15] demonstrated that acetylation of lysine residues of p53 promotes neurite outgrowth and transactivation of *GAP-43* gene. In our study, a remarkable reduction of GAP-43 mRNA and protein levels were found in SY5Y-APP clone. This observations agree with those studies in which very low levels of GAP-43 mRNA were found in cortical neurons of postmortem AD brain in comparison with control slices, as wells as in APP-transgenic mice.[27–29]

The decrease of GAP-43 expression in SY5Y-APP cells was essentially due to the impairment of p53 activity. This was well demonstrated by ChIP assay, which showed that in basal conditions p53 was mostly in unfolded conformation and did not occupy GAP-43 promoter. However, after zinc supplementation, p53 rescued its wild-type conformation and bind GAP-43 promoter region.

We speculated that the decreased expression of GAP-43 in SY5Y-APP clone may compromise neuronal plasticity, as the protein has a key role in regulating axonal growth-cone.[17] This hypothesis was supported essentially by the evidence that only when SY5Y-APP cells were differentiated by RA in the presence of zinc chloride (that reverted p53wt state), extensive growth-cone area, GAP-43 positive, was observed. According with our observations, Qin *et al.*,[16] showed that treatment of primary cortical neurons with specific p53 inhibitors or expressing a p53-R175H-mutant caused growth-cone collapse.

Thus, we propose the following molecular-cascade (Figure 8): elevated oxidative environment affects p53 conformation towards an unfolded structure. In this unfolded state, p53 is not able to exert its proapototic activity and physiological role in axonal outgrowth.

Material and Methods

Cell culture and transfections. Human neuroblastoma cell line SH-SY5Y was cultured in Ham's F12 and Dulbecco modified Eagle's medium in a ratio of 1 : 1, supplemented with 10% (v/v) fetal calf serum, 2 mM glutamine, 50 μg/ml penicillin and 100 μg/ml streptomycin and kept at 37 °C in humidified 5% CO_2/95% atmosphere.

SY5Y-APP cells steadily transfected with APP 751 wt were prepared as follows. SH-SY5Y cells, seeded on polylysine-coated six-well plate at 80% of confluence density, were transfected with 1 μg/well of pcDNA–APP751 vector using Lipofectamine 2000 reagent (Invitrogen, Milan, Italy). G418 (Sigma-Aldrich, St Louis, MO, USA) was added at a concentration of 800 μg/ml and drug resistant cells were collected after 2–3 weeks for single-cell cloning, in 96-well plates. Wells containing more than one cell were marked and excluded from further investigation. Fifty percent of the medium in each well was replaced twice a week. After 4–6 weeks, surviving clones reached confluency and were expanded for banking. Resistant clones were analyzed by western blot to confirm the overexpression of APP. Steadily transfected cells expressing APP construct were maintained in G418 at a final concentration of 600 μg/ml.

H_2O_2 treatment and evaluation of cell viability. SH-SY5Y empty vector-transected cells (mock) and SY5Y-APP cells were exposed to H_2O_2. Briefly, cells were washed with phosphate buffer saline (PBS) and treated with 1 mM H_2O_2 for 5 min. After washing, cells were returned to full fresh medium for 24 h. Cell viability was measured by quantitative colorimetric assay, using 500 μg/ml of MTT (3-(4,5-dimethylthiazol-2-yl)-2,5-diphenyltetrazolium bromide) on cells incubated at 37 °C for 3 h. MTT was removed and cells were lysed with dimethyl sulfoxide. The absorbance at 595 nm was measured using a Bio-Rad 3350 microplate reader (Bio Rad Laboratories, Richmond, CA, USA). Control cells were treated in the same way without H_2O_2, and the values of different absorbance were expressed as a percentage of control.

Western blot analysis. Cells were harvested in 80 μl of lysis buffer containing 50 mM Tris-HCl (pH 7.6), 150 mM NaCl, 5 mM EDTA, 1 mM phenyl methyl sulphonyl fluoride, 0.5 μg/μl leupeptin, 5 μg/μl aprotinin and 1 μg/ml pepstatin. Protein content was determined by a conventional method (BCA protein assay kit, Pierce, Rockford, IL, USA). Thirty microgram of protein extracts were electrophoresed on 12% SDS-PAGE and transferred to nitrocellulose paper (Schleicher and Schuell, Dassel, Germany). Filters were incubated at 4 °C overnight with different primary antibodies diluted in 5% non-fat dried milk. For APP protein and its processing products, the following antibodies were used: an antibody recognized the N-terminus domain of APP protein (22C11, 1 : 150, Chemicon Millipore, Billerica, MA, USA), the antibody 6E10, direct towards the fragment 1–17 of Aβ (1 : 200, Sigma-Aldrich), and a C-terminus antibody, against the nine amino acid from the C-terminus of APP (1 : 250, Sigma-Aldrich). Other antibodies used: anti-p53 (1 : 1000, Novocastra, Newcastle, UK), anti-p21/WAF1 (1 : 200, Novocastra), anti-GAP-43 (1 : 1500 Chemicon Millipore), and anti-βIII-tubulin (1 : 2000, Chemicon Millipore), anti-nucleolin (1 : 2000, Santa Cruz Biotechnology, Santa Cruz, CA, USA). The secondary antibodies (Santa Cruz Biotechnology) and a chemiluminescence blotting substrate kit (Boehringer, Mannheim, Germany) were used for immunodetection.

Analysis of p53 conformational state. p53 conformational state was analyzed by immunopreciptation experiment and ELISA, using the conformational specific anti-p53 antibodies, PAb1620 and PAb240. In particular, cells were lysed in immunoprecipitation buffer (10 mM Tris, pH 7.6; 140 mM NaCl; and 0.5% NP40 including protease inhibitors) for 20 min on ice, and cell debris were cleared by centrifugation. Protein content was determined by a conventional method (BCA protein assay Kit, Pierce). Before immunoprecipitation experiments, an aliquot of 10 μg of protein extracts from each individual sample was processed for western blot analysis and probed with anti-α tubulin antibody to validate protein content measurements (data not shown). Based on the previous results, 100μg of protein extracts were used for immunoprecipitation experiments, performed in a volume of 500 μl. To prevent nonspecific binding, the supernatant of immunoprecipitated samples was precleared with 10% (w/v) protein A/G (50 μl) (SantaCruz Biotechnology Inc., Heidelberg, Germany) for 20 min on ice, followed by centrifugation. For immunoprecipitation of p53, 1 μg of the conformation-specific antibodies PAb1620 (wild-type specific) (Calbiochem, EMB Bioscience, La Jolla, CA, USA) or PAb240 (mutant specific) (Neomarkers-Lab Vision, Fremont, CA, USA) were added to the samples and incubated overnight at 4 °C. Immunocomplexes were collected by using protein A/G suspension and washed five times with immunoprecipitation buffer. Immunoprecipitated p53 was recovered by resuspending pellets in Laemmli sample buffer. Western blot analysis was performed using as primary antibodies:polyclonal anti-p53 antibody R19 (SantaCruz Biotechnology Inc.), polyclonal anti-HNE and polyclonal anti-3NT antibodies. For ELISA assay 70 μg of non-denaturated protein extracts were diluted in PBS 1 × pH 7.4 and coated on the ELISA microplate overnight at 4 °C. The next day plates were saturated with 100 μl of blocking solution (PBS 1 × pH 7.4–0.1% TWEEN 20–3% bovine serum albumin (BSA)) for each well and incubated for 1 h at room temperature, followed by 2 h incubated at 37 °C with anti-p53 PAb240 antibody (0.5 μg/ml) and Pab1620 (0.5 μg/ml). After washing with PBST (PBS 1 × pH 7.4–0.5% TWEEN 20), 0.1 mg/ml secondary anti-mouse antibody conjugated with peroxidase was incubated in each well for 1 h at room temperature. Finally, 100 μl of TMB (3,3,5,5-tetramethylbenzidine) substrate was added and the reaction is stopped with 100 μl of sulfuric acid 2 M. Optical density was measured using a microplate reader with a wavelength of 450 nm. Data were expressed as the mean ± S.E. of at least three experiments, performed in triplicate.

Immunofluorescence and confocal analysis. Cells were plated at a density of 5×10^4 cells/cm^2 in a 24-well plate, grown on glass coverslip (coated with poly-D-lysine; Sigma-Aldrich) and then fixed. Cells were incubated in PBS (Sigma-Aldrich) containing 1% BSA (Sigma-Aldrich) and 0.2% Triton X-100

overnight at 4 °C with the appropriate antibody. After rinsing, cells were incubated with the secondary antibody in PBS for 1 h at room temperature. Slices were mounted using the Dako Fluorescent Mounting Medium and examined by Zeiss LSM 510 META confocal laser-scanning microscope (Carl Zeiss Inc, Thornwood, NY, USA). Antibodies used for immunocytochemistry were the following: anti-GAP-43 (1 : 5000, Chemicon Millipore), anti-βIII tubulin (1 : 200, Chemicon Millipore), a specific Aβ42 polyclonal antibody (1 : 100, Biosource, Carlsbad, CA, USA). Secondary antibodies used were: anti-mouse CY3 (1 : 500, Invitrogen) and anti-rabbit Alexa Fluor-conjugated (1 : 500 Invitrogen).

Measurement of oxidative stress markers. Nitro-tyrosine content and measurement of 4-hydroxynonenal (HNE) were determined immunochemically, as previously described.[58,59] Briefly, samples were incubated in Laemmli sample buffer in a 1 : 2 ratio (0.125 M Trizma base, pH 6.8, 4% sodium dodecyl sulfate, 20% glycerol) for 20 min. Proteins (5 μg) were then blotted onto the nitrocellulose paper using the slot-blot apparatus and immunochemical analysis was performed. The primary anti-3NT antibody (Sigma-Aldrich) diluted 1 : 1000, and anti-HNE polyclonal antibody (Alpha Diagnostic International Inc., San Antonio, TX, USA) diluted 1 : 200 were incubated at 4 °C over night, followed by 3 h at room temperature and then HRP-conjugated goat anti-rabbit antibody (1 : 1500 Dako, Glostrup, Denmark) at room temperature for 2 h was used for detection. Alfa-tubulin was used to normalize the sample content. Quantitative analysis was performed with Scion Image.

Quantitative real-time PCR. One microgram of total RNA from mock and SY5Y-APP cells was transcribed into cDNA using murine leukemia virus reverse transcriptase (Promega, Madison, WI, USA) and oligo-dT (15–18) as a primer (final volume, 50 μl). Parallel reactions containing no reverse transcriptase were used as negative controls to confirm the removal of all genomic DNA. Human-specific primers were designed using the Primer3 software (http://frodo.wi.mit.edu).[60] The oligonucleotide sequences of the primers (M-Medical) used are as follows: GAP-43, forward primer, 5′-TTC TTG GTG TTG TTA TGG CAA G-3′, reverse primer, 5′-GAG GAA AGT GGA CTC CCA CAG-3′; APP, forward primer, 5′-AAG AAG GCA GTT ATC CAG CAT TTC-3′, reverse primer, 5′-TTG TAG AGC AGG GAG AGA GAC TGA-3′, GAPDH, forward primer, 5′-GAG TCA ACG GAT TTG GTC GT-3′, reverse primer, 5′-TTG ATT TTG GAG GGA TCT CG-3′. Amplification and detection were performed with the iCYCLER iQ quantitative real-time PCR (Q-RT-PCR) Detection System (Bio-Rad); the fluorescence signal was generated by SYBR Green I. Samples were run in triplicate in a 25 μl of reaction mix containing 12.5 μl of 2 $\times$ SYBR Green Master Mix (Bio-Rad), 12.5 pmol of each forward and reverse primer and 2 μl of diluted cDNA. Each PCR experiment included serial dilutions of a positive control for construction of the calibration curve, a positive and a negative DNA sample and water blanks. The PCR program was initiated by 10 min at 95 °C followed by 40 cycles, each one of 15 s at 95 °C and 1 min at 56–62 °C. A subsequent dissociation curve analysis verified the Ct for the target gene minus the mean of the Ct for the internal control gene. The Ct represented the mean difference between the Ct of the test minus the Ct of the calibrator. The N-fold differential expression in the target gene of the test compared with calibrator was expressed as $2^{-\Delta\Delta Ct}$. Data analysis and graphics were performed using GraphPad Prism 4 software (GraphPad, San Diego, CA, USA) and were the results of at least three different experiments run in triplicate for each gene.

Transactivation assay. Transient transfections were performed in six multi-well culture plates, for each well 7×10^5 cells were seeded in medium without FBS, antibiotics and with 1% L-glutamine. For transactivation, assay cells were transfected with the p53-target promoter AIP1-luciferase reporter plasmid (kindly provided by H Arakawa, National Cancer Center, Tokyo, Japan), by using the transfection reagent LTX (Invitrogen, Carlsbad, CA, USA) according to the manufacturer's instructions. AIP1-luciferase reporter construct plasmid DNA was co-transfected with pRL-TK Renilla luciferase expressing vector to measure transfection efficiency (Promega). Eighteen hours later the cells were incubated with 50 μM doxorubicin for 24 h before luciferase activity was assayed. The cells were then lysed with passive lysis buffer 1 $\times$ provided by Dual-Luciferase Reporter Assay System following the manufacturer's specifications (Promega). Luminescence was measured employing a 20/20n Luminometer with 10 s of integration (Turner BioSystems, Sunnyvale, CA, USA). At least six independent experiments were performed.

Chromatin immunoprecipitation analysis. Chromatin immunoprecipitation (ChIP) analysis was performed as described by Lanni *et al.*[61] Protein complexes were crosslinked to DNA in living cells by adding formaldehyde directly to the cell culture medium at 1% final concentration. Chromatin extracts containing DNA fragments with an average size of 300 bp were incubated overnight at 4 °C with milk shaking using polyclonal rabbit polyclonal anti-p53 antibody (FL-393, Santa Cruz), as described by Tedeschi *et al.*[15] DNA–protein complexes were recovered with protein A/G-agarose (Santa Cruz). Before use, protein A/G was blocked with 1 μg/μl sheared herring sperm DNA and 1 μg/μl BSA overnight at 4 °C, and then incubated with chromatin and antibodies for 3 h at 4 °C. PCR was performed using immunoprecipitated DNA and promoter-specific primers flanking the p53 site for GAP-43 (M-Medical) and specific primers for GAPDH, used as housekeeping gene. Primer sequences used were as follows: GAP-43 promoter, forward primer, 5′-CCT CTT TAG AAA TAG CTG TTC TTT GC-3′, reverse primer, 5′-TAA ACA CCT CCA ATC TGG ACC-3′; GAPDH, forward primer, 5′-GAG TCA ACG GAT TTG GTC GT -3′, reverse primer, 5′-TTG ATT TTG GAG GGA TCT CG-3′. Immunoprecipitation with nonspecific Igs (no Ab) was performed as negative controls. PCR products were run on a 2.5% agarose gel and visualized with ethidium bromide staining using UV light. The amount of precipitated chromatin measured in each PCR was normalized with the amount of chromatin present in the input of each immunoprecipitation.

Statistical analysis. Results are given as mean ± S.E.M. values. Statistical significance of differences was determined by mean values of both the *t*-test and one-way ANOVA, followed by the Bonferroni test. Significance was accepted for a $P < 0.05$.

Conflict of Interest

The authors declare no conflict of interest.

Acknowledgements. This work was supported by Ministero dell'Università e della Ricerca (grants 2008R25HBW_004 to D. L. U. and 2009B7ASKP_006 to M. M.) and by grant from Regione Lombardia 'Network Enable Drug Design' (NEDD).

1. Tolstonog GV, Deppert W. Metabolic sensing by p53: keeping the balance between life and death. *Proc Natl Acad Sci U S A.* 2010; **107**: 13193–13194.
2. Brady CA, Attardi LD. p53 at a glance. *J Cell Sci* 2010; **123**: 2527–2532.
3. Levine AJ. p53, the cellular gatekeeper for growth and division. *Cell* 1997; **88**: 323–331.
4. Kaya SS, Mahmood A, Li Y, Yavuz E, Goksel M, Chopp M. Apoptosis and expression of p53 response proteins and cyclin D1 after cortical impact in rat brain. *Brain Res* 1999; **818**: 23–33.
5. Crumrine RC, Thomas AL, Morgan PF. Attenuation of p53 expression protects against focal ischemic damage in transgenic mice. *J Cereb Blood Flow Metab* 1994; **14**: 887–891.
6. Hughes PE, Alexi T, Yoshida T, Schreiber SS, Knusel B. Excitotoxic lesion of rat brain with quinolinic acid induces expression of p53 messenger RNA and protein and p53-inducible genes Bax and Gadd-45 in brain areas showing DNA fragmentation. *Neuroscience* 1996; **74**: 1143–1160.
7. Medrano S, Scrable H. Maintaining appearances–the role of p53 in adult neurogenesis. *Biochem Biophys Res Commun* 2005; **331**: 828–833.
8. Culmsee C, Mattson MP. p53 in neuronal apoptosis. *Biochem Biophys Res Commun* 2005; **331**: 761–777.
9. Hughes PE, Alexi T, Schreiber SS. A role for the tumour suppressor gene p53 in regulating neuronal apoptosis. *Neuroreport* 1997; **8**: v–xii.
10. Morrison RS, Wenzel HJ, Kinoshita Y, Robbins CA, Donehower LA, Schwartzkroin PA. Loss of the p53 tumor suppressor gene protects neurons from kainate-induced cell death. *J Neurosci* 1996; **16**: 1337–1345.
11. Uberti D, Belloni M, Grilli M, Spano P, Memo M. Induction of tumour-suppressor phosphoprotein p53 in the apoptosis of cultured rat cerebellar neurones triggered by excitatory amino acids. *Eur J Neurosci* 1998; **10**: 246–254.
12. Li Y, Chopp M, Zhang ZG, Zaloga C, Niewenhuis L, Gautam S. p53-immunoreactive protein and p53 mRNA expression after transient middle cerebral artery occlusion in rats. *Stroke* 1994; **25**: 849–855; (discussion 55-6).
13. Morrison RS, Kinoshita Y, Johnson MD, Guo W, Garden GA. p53-dependent cell death signaling in neurons. *Neurochem Res* 2003; **28**: 15–27.
14. Culmsee C, Zhu X, Yu QS, Chan SL, Camandola S, Guo Z *et al.* A synthetic inhibitor of p53 protects neurons against death induced by ischemic and excitotoxic insults, and amyloid beta-peptide. *J Neurochem* 2001; **77**: 220–228.
15. Tedeschi A, Nguyen T, Puttagunta R, Gaub P, Di Giovanni SA. p53-CBP/p300 transcription module is required for GAP-43 expression, axon outgrowth, and regeneration. *Cell Death Differ* 2009; **16**: 543–554.

16. Qin Q, Baudry M, Liao G, Noniyev A, Galeano J, Bi X. A novel function for p53: regulation of growth cone motility through interaction with Rho kinase. *J. Neurosci* 2009; **29**: 5183–5192.
17. Denny JB. Molecular mechanisms, biological actions, and neuropharmacology of the growth-associated protein GAP-43. *Curr Neuropharmacol* 2006; **4**: 293–304.
18. Aarts LH, Schotman P, Verhaagen J, Schrama LH, Gispen WH. The role of the neural growth associated protein B-50/GAP-43 in morphogenesis. *Adv Exp Med Biol* 1998; **446**: 85–106.
19. Bendotti C, Baldessari S, Pende M, Southgate T, Guglielmetti F, Samanin R. Relationship between GAP-43 expression in the dentate gyrus and synaptic reorganization of hippocampal mossy fibres in rats treated with kainic acid. *Eur J Neurosci* 1997; **9**: 93–101.
20. Uberti D, Lanni C, Carsana T, Francisconi S, Missale C, Racchi M *et al.* Identification of a mutant-like conformation of p53 in fibroblasts from sporadic Alzheimer's disease patients. *Neurobiol Aging* 2006; **27**: 1193–1201.
21. Lanni C, Racchi M, Stanga S, Mazzini G, Ranzenigo A, Polotti R *et al.* Unfolded p53 in blood as a predictive signature signature of the transition from mild cognitive impairment to Alzheimer's disease. *J Alzheimers Dis* 2010; **20**: 97–104.
22. Lanni C, Racchi M, Mazzini G, Ranzenigo A, Polotti R, Sinforiani E *et al.* Conformationally altered p53: a novel Alzheimer's disease marker? *Mol Psychiatry* 2008; **13**: 641–647.
23. Serrano J, Fernandez AP, Martinez-Murillo R, Martinez A. High sensitivity to carcinogens in the brain of a mouse model of Alzheimer's disease. *Oncogene* 2010; **29**: 2165–2171.
24. Chetelat G, Villemagne VL, Pike KE, Ellis KA, Ames D, Masters CL *et al.* Relationship between memory performance and beta-amyloid deposition at different stages of Alzheimer's disease. *Neurodegener Dis* 2012; **10**: 141–144.
25. Shankar GM, Li S, Mehta TH, Garcia-Munoz A, Shepardson NE, Smith I *et al.* Amyloid-beta protein dimers isolated directly from Alzheimer's brains impair synaptic plasticity and memory. *Nat Med* 2008; **14**: 837–842.
26. Wu L, Rosa-Neto P, Hsiung GY, Sadovnick AD, Masellis M, Black SE *et al.* Early-onset familial Alzheimer's disease (EOFAD). *Can J Neurol Sci* 2012; **39**: 436–445.
27. Hartl D, Rohe M, Mao L, Staufenbiel M, Zabel C, Klose J. Impairment of adolescent hippocampal plasticity in a mouse model for Alzheimer's disease precedes disease phenotype. *PLoS One* 2008; **3**: e2759.
28. de la Monte SM, Ng SC, Hsu DW. Aberrant GAP-43 gene expression in Alzheimer's disease. *Am J Pathol* 1995; **147**: 934–946.
29. Coleman PD, Kazee AM, Lapham L, Eskin T, Rogers K. Reduced GAP-43 message levels are associated with increased neurofibrillary tangle density in the frontal association cortex (area 9) in Alzheimer's disease. *Neurobiol Aging* 1992; **13**: 631–639.
30. Tsuzuki K, Fukatsu R, Takamaru Y, Fujii N, Takahata N. Potentially amyloidogenic fragment of 50 kDa and intracellular processing of amyloid precursor protein in cells cultured under leupeptin. *Brain Res* 1994; **659**: 213–220.
31. Multhaup G, Scheuermann S, Schlicksupp A, Simons A, Strauss M, Kemmling A *et al.* Possible mechanisms of APP-mediated oxidative stress in Alzheimer's disease. *Free Radic Biol Med* 2002; **33**: 45–51.
32. Uchida K. Histidine and lysine as targets of oxidative modification. *Amino Acids* 2003; **25**: 249–257.
33. Sultana R, Butterfield DA. Proteomics identification of carbonylated and HNE-bound brain proteins in Alzheimer's disease. *Methods Mol Biol* 2009; **566**: 123–135.
34. Hainaut P, Milner J. Redox modulation of p53 conformation and sequence-specific DNA binding in vitro. *Cancer Res* 1993; **53**: 4469–4473.
35. Buizza L, Cenini G, Lanni C, Ferrari-Toninelli G, Prandelli C, Govoni S *et al.* Conformational altered p53 as an early marker of oxidative stress in Alzheimer's disease. *PLoS One* 2012; **7**: e29789.
36. Meplan C, Richard MJ, Hainaut P. Redox signalling and transition metals in the control of the p53 pathway. *Biochem Pharmacol* 2000; **59**: 25–33.
37. Tedeschi A, Di Giovanni S. The non-apoptotic role of p53 in neuronal biology: enlightening the dark side of the moon. *EMBO Rep* 2009; **10**: 576–583.
38. Di Giovanni S, Rathore K. p53-dependent pathways in neurite outgrowth and axonal regeneration. *Cell Tissue Res* 2012; **349**: 87–95.
39. Di Giovanni S, Knights CD, Rao M, Yakovlev A, Beers J, Catania J *et al.* The tumor suppressor protein p53 is required for neurite outgrowth and axon regeneration. *EMBO J* 2006; **25**: 4084–4096.
40. Eizenberg O, Faber-Elman A, Gottlieb E, Oren M, Rotter V, Schwartz M. p53 plays a regulatory role in differentiation and apoptosis of central nervous system-associated cells. *Mol Cell Biol* 1996; **16**: 5178–5185.
41. Meplan C, Richard MJ, Hainaut P. Metalloregulation of the tumor suppressor protein p53: zinc mediates the renaturation of p53 after exposure to metal chelators in vitro and in intact cells. *Oncogene* 2000; **19**: 5227–5236.
42. Ondrejcak T, Klyubin I, Hu NW, Barry AE, Cullen WK, Rowan MJ. Alzheimer's disease amyloid beta-protein and synaptic function. *Neuromolecular Med* 2010; **12**: 13–26.
43. Johnston H, Boutin H, Allan SM. Assessing the contribution of inflammation in models of Alzheimer's disease. *Biochem Soc Trans* 2011; **39**: 886–890.
44. Galimberti D, Scarpini E. Inflammation and oxidative damage in Alzheimer's disease: friend or foe? *Front Biosci (Schol Ed)* 2011; **3**: 252–266.
45. Sultana R, Butterfield DA. Role of oxidative stress in the progression of Alzheimer's disease. *J Alzheimers Dis* 2010; **19**: 341–353.
46. Cai Z, Zhao B, Ratka A. Oxidative stress and beta-amyloid protein in Alzheimer's disease. *Neuromolecular Med* 2011; **13**: 223–250.
47. Uberti D, Cenini G, Olivari L, Ferrari-Toninelli G, Porrello E, Cecchi C *et al.* Over-expression of amyloid precursor protein in HEK cells alters p53 conformational state and protects against doxorubicin. *J Neurochem* 2007; **103**: 322–333.
48. Cenini G, Maccarinelli G, Lanni C, Bonini SA, Ferrari-Toninelli G, Govoni S *et al.* Wild type but not mutant APP is involved in protective adaptive responses against oxidants. *Amino Acids* 2010; **39**: 271–283.
49. Lanni C, Uberti D, Racchi M, Govoni S, Memo M. Unfolded p53: a potential biomarker for Alzheimer's disease. *J Alzheimers Dis* 2007; **12**: 93–99.
50. Velu CS, Niture SK, Doneanu CE, Pattabiraman N, Srivenugopal KS. Human p53 is inhibited by glutathionylation of cysteines present in the proximal DNA-Binding domain during oxidative stress. *Biochemistry* 2007; **46**: 7765–7780.
51. Calmels S, Hainaut P, Ohshima H. Nitric oxide induces conformational and functional modifications of wild-type p53 tumor suppressor protein. *Cancer Res* 1997; **57**: 3365–3369.
52. Willis A, Jung EJ, Wakefield T, Chen X. Mutant p53 exerts a dominant negative effect by preventing wild-type p53 from binding to the promoter of its target genes. *Oncogene* 2004; **23**: 2330–2338.
53. Tsvetkov P, Reuven N, Shaul Y. Ubiquitin-independent p53 proteasomal degradation. *Cell Death Differ* 2010; **17**: 103–108.
54. Cregan SP, MacLaurin JG, Craig CG, Robertson GS, Nicholson DW, Park DS *et al.* Bax-dependent caspase-3 activation is a key determinant in p53-induced apoptosis in neurons. *J Neurosci* 1999; **19**: 7860–7869.
55. Xu X, Yang D, Wyss-Coray T, Yan J, Gan L, Sun Y *et al.* Wild-type but not Alzheimer-mutant amyloid precursor protein confers resistance against p53-mediated apoptosis. *Proc Natl Acad Sci U S A.* 1999; **96**: 7547–7552.
56. Lanni C, Racchi M, Memo M, Govoni S, Uberti D. p53 at the crossroads between cancer and neurodegeneration. *Free Radic Biol Med* 2012; **52**: 1727–1733.
57. Sun XZ, Vinci C, Makmura L, Han SB, Tran D, Nguyen J *et al.* Formation of disulfide bond in p53 correlates with inhibition of DNA binding and tetramerization. *Antioxid Redox Sign* 2003; **5**: 655–665.
58. Drake J, Sultana R, Aksenova M, Calabrese V, Butterfield DA. Elevation of mitochondrial glutathione by gamma-glutamylcysteine ethyl ester protects mitochondria against peroxynitrite-induced oxidative stress. *J Neurosci Res* 2003; **74**: 917–927.
59. Lauderback CM, Hackett JM, Huang FF, Keller JN, Szweda LI, Markesbery WR *et al.* The glial glutamate transporter, GLT-1, is oxidatively modified by 4-hydroxy-2-nonenal in the Alzheimer's disease brain: the role of Abeta1-42. *J Neurochem* 2001; **78**: 413–416.
60. Rozen SL, Skaletsky HJ. Primer3 on the WWW for general users and for biologist programmers. In: Krawetz S, Misener S (eds) *Bioinformatics Methods and Protocols: Methods in Molecular Biology*. Humana Press: Totowa, NJ, 2000, pp 365–386.
61. Lanni C, Nardinocchi L, Puca R, Stanga S, Uberti D, Memo M *et al.* Homeodomain interacting protein kinase 2: a target for Alzheimer's beta amyloid leading to misfolded p53 and inappropriate cell survival. *PLoS One* 2010; **5**: e10171.

Supplementary Information accompanies the paper on Cell Death and Disease website (http://www.nature.com/cddis)